Original Article

pISSN, eISSN 0125-5614
M Dent J 2020; 40 (2) : 95-106

Topography alteration of different implant surfaces after an installation

Sakanus Vijintanawan[1], Teeranut Chaiyasamut[1], **Suphachai Suphangul**[2], Natthamet Wongsirichat[1]

[1] *Department of Oral Maxillofacial Surgery, Faculty of Dentistry, Mahidol University*
[2] *Department of Advanced General Dentistry, Faculty of Dentistry, Mahidol University*

Objective: The aims of present study were to investigate dental implant surface alterations after the installation.
Materials and methods: Four types of implant with different surface modification (sandblasted and acid-etched (SLA), SLA with nano-apatite coating, laser, and anodized surface) were assigned to control and test groups (n=5). The installation was performed in porcine bone. Consequently, the implant surfaces were investigated with scanning electron microscope and confocal laser microscope to identify micro topographical change.
Results: Morphological alterations were found in all test implants such as thread abrasion, flattening area, crack, and decreased surface projection. Topographical analysis showed that arithmetical mean height and surface area significantly decreased in all test groups (2-20% and 3-6%, respectively). Surface skewness of SLA significantly increased after installation. Surface kurtosis and texture aspect ratio remained the same.
Conclusions: All implant surfaces exhibited the surface alteration after the installation. The anodized implant was the least change. SLA implant presented the greatest surface change after the installation.

Keywords: implant surface, surface alteration, topography

How to cite: Vijintanawan S, Cahiyasamut T, Suphangul S, Wongsirichat N. Topography alteration of different implant surfaces after an installation. M Dent J 2020; 40: 95-106.

Introduction

In oral implantology, researchers have developed macroscopic and microscopic designs continuously. The macroscopic design of shape and thread influences an insertion force, mechanical retention, and occlusal force distribution [1-4]. Meanwhile, the microscopic design, defined as surface roughness, is responsible for reliable osseointegration [5,6]. Surface roughness is described by first, a morphology under a scanning electron microscope (SEM) and second, numerical topographic data from a profilometer, interferometer, confocal microscope, or atomic force microscope [7]. Surface modification, such as sandblasted and acid-etched surface, anodized surface, and laser treatment, provides optimal surface roughness and encourages a physico-chemical interaction, strong cell response and clinical success [5,8-10].

During installation of the dental implant, stress concentrates at different areas over the implant surface, depending on a bone density, implant design, and osteotomy regimen [11]. Shear force is an occurrence during installation that causes implant surface abrasion and surrounding bone damage [12,13]. The current

Correspondence author: Suphachai Suphangul
Department of Advanced General Dentistry, Faculty of Dentistry, Mahidol University
6 Yothi Road, Ratchathewi District, Bangkok 10400 Thailand
E-mail: kungomfs@gmail.com
Received : 10 April 2020 Accepted : 25 June 2020

study questions whether there are surface changes after installation. Moreover, oral implant studies always relate topographical information of unblemished implant to various factors such as cell response, hydrophilicity. The present study views that this might not be relevant to the clinical scenario since the implant surface might have already altered after installation process. Previous studies have not drawn conclusion if any significant surface damage is presented after installation. Most studies reported the alterations, for example cracked, smoothened, chipped surface, and altered roughness parameter [13-17].

The present study aims to investigate the surface alteration. The null hypothesis is that there is no alteration of surface character and topography after installation.

Materials and methods

Experimental model

The experiment was carried out on an ex vivo porcine pelvis model. The bones were prepared into blocks before an implant placement. The implants were assessed having a micro-level surface roughness.

Bone block preparation

Ilium of porcine lesser pelvic were sectioned using a precision sectioning saw (Low speed saw, Buehler, Illinois, USA) with a copious normal saline irrigation to approximately 2 cm cubic blocks. The cubical bones were sent to a radiographic examination using a computed tomography (CT; Revolution frontier, GE Health Care Co., Inc., Chicago, USA). Dicom files were transferred to software coDiagnostiX (Dental Wings Inc., Basel, Switzerland) to verify Hounsfield unit of each block. A simulated implant placement at the center of the blocks was done then average bone densities were measured as Hounsfield unit (Hu) within implant area. The cortical bone thicknesses were measured as well. The blocks were random to each test group using stratified random sampling based on the cortical thickness and Hu. The bone blocks were also split into halves and clamped to prevent the damage during implant removal.

Test and control groups

Forty implants from four companies were selected including Superline (SU, Dentium, Seoul, Korea), TSIII BA (TS, Osstem, Seoul, Korea), Biomate Plus (BP, Biomate, Kaohsiung, Taiwan), and Nobel CC (NO, Nobel Biocare, Karlskoga, Sweden). Detailed implants characteristics are listed in (Table 1). All implants were grade IV titanium. Ten implants of each brand were allocated into each test and control groups (n=5). In test group, the implants were installed and cleaned before surface investigation. In control group, the implants were only cleaned with the same protocol as test group before the investigation.

Table 1 Dental implants

Implants	Size	Surface
SU	4.0 x 10 mm	Sandblasted large-grit acid-etched (SLA)
TS	4.0 x 10 mm	SLA with apatite nano-coating surface
BP	4.0 x 10 mm	Laser treated surface
NO	4.3 x 10 mm	Anodized surface

Remark: SU: (Superline, Dentium, Seoul, Korea)
TS: (TSIII BA, Osstem, Seoul, Korea)
BP: (Biomate Plus, Biomate, Kaohsiung, Taiwan)
NO: (Nobel CC, Nobel Biocare, Karlskoga, Sweden)

Implant bed preparation and installation

Implant bed preparation was performed by a single skillful clinician who followed the manufacture recommendations using a surgical micromotor control unit (iCT motor, Dentium, Seoul, Korea). The implants were inserted equicrestally, then impression coping was placed. Consequently, the block was unclamped and separated into halves, then the implant was carefully removed by holding the impression copings and avoiding contact with the implant surfaces. The implant was easily detached from surrounding bone. All torque values from a motor torque recognition were recorded during installation.

Microscopic and topographic investigation

All implants from the test and control groups were sonicated using an ultrasonic bath (Vibraclean300, MDT Corporation, California, USA) filled with distilled water for 1 hour and acetone for 1 hour. The implants did not contact the ultrasonic bath surface during the cleaning process to prevent unintentional surface damage. The implants were removed from acetone and kept in a desiccator for 24 hours before beginning microscopic and topographic investigations.

Scanning electron microscope

Scanning electron microscope (SEM) (JSM-6610LV, Jeol USA Inc., Massachusetts, USA) assessed surface morphology at thread top, flank, and valley over the implant body. General surface appearance and any surface alterations were described.

Surface topography

Confocal laser microscope (CLM) (Nanosearch Ols4500, Shimadzu Co., Kyoto, Japan) was used to randomly illustrate twenty-seven 3D surface images of thread top, flank, and valley at coronal, middle, and apical parts surrounding the implant body. The region of interest was aligned perpendicular to a laser beam. 20x objective lens, 1.5 mm focus range with 8x magnification provided 80x80 μm images. The images were processed using software Lext1.1.3 (Olympus, Tokyo, Japan). Noise removal and Gaussian filtering of 50 μm-cutoff were applied. The topographical parameters; surface area: area ratio (S-ratio), arithmetical mean height (Sa), surface kurtosis (Sku), surface skewness (Ssk), and texture aspect ratio (Str) were obtained. Definition of parameters are shown in (Table 2).

Table 2 Parameter definitions

Parameters	Definition
S-ratio	True surface area/cross sectional area. Increased number indicates increased micro surface area from surface modification.
Sa	Absolute value of difference in height of each point compared to the arithmetical mean plane. The greater value indicates deep grooves or sharp asperities construction.
Ssk	Representation of degree of symmetry of the surface heights about the mean plane. The sign of Ssk indicates the predominance of peaks when Ssk > 0 or valley structures when Ssk <0 comprising the surface.
Sku	Representation of inordinately high peaks or deep valleys when Sku > 3.00. Surfaces which are gradually varying and free of extreme peaks or valley features, tend to have Sku < 3.00.
Str	Identification of texture pattern. The texture aspect ratio has a value between 0 and 1. Larger values, Str > 0.5 indicates stronger uniform texture aspect in directions, whereas smaller values, Str < 0.3, indicates stronger long-crestness.

Statistical analysis

Statistical analyses were performed using the commercially available software, SPSS version 18.0 (Statistical package for the social sciences, SPSS, Chicago, IL, USA). The data normality was proved using the Kolmogorov-Smirnov test. The Hu, cortical bone thicknesses, torque values, and all parameters were expressed as the mean ± standard deviation (SD). Difference between groups were analyzed by one-way analysis of variance (ANOVA) and Tukey test. The *t* test was used for control-test group comparison. The statistical significance level was set to $P < 0.05$.

Results

Bone block evaluation and insertion torque values

Hu, cortical bone thicknesses, and insertion torque values are presented in (Table 3). The mean Hu and cortical bone thicknesses were 580.57 ± 21.4 and 2.397 ± 0.25 mm, respectively. Hu and cortical bone thicknesses were found to be statistically insignificant difference between groups ($P = 1$ and .904). The mean insertion torque was 31.80 ± 2.3 Ncm. The insertion torque values in all groups were found to have statistically insignificant difference between groups ($P = 0.821$).

Scanning electron microscope

All implants were tapered design and consisted of different thread shapes. Cleaning protocol could eliminate debris over implant surface and reveal surface morphology clearly. Each implant demonstrated exclusive surface character.

SU presented triangle-shaped thread. SEM image demonstrated a spike-like structure and porosity which presented smaller pores within larger pores. The smallest pore could be identified in submicron level. Surface morphology seemed isotropic and homogeneous over the total surface (Figure 1).

TS was similar to SU which presented the triangular threads, spike-like structure and porosity. However, surface morphology of TS consisted of deeper and larger crater from blasting process. Moreover, nano hydroxyapatite coating was visually removed after cleaning protocol (Figure 1).

After installation, both SU and TS exhibited similar outcome. Top of the thread, especially coronal and apical part presented smoothening area varying from submicron to micron in size. The spike-like structure decreased sharpness. Some thread crests became blunter. Flank and valley areas rarely changed (Figure 2).

BP surface showed trapezoid-shaped thread. SEM image revealed 2 levels of roughness; first, a homogeneous groovy pattern continued from coronal to apical part along the long axis of the implant, considered as anisotropic surface texture. Each groovy unit consisted top (10-15 μm-width), cliff, and valley (10-15 μm-width). Second, the image revealed submicron knobby-like pattern over the surface, considered as submicron and nano roughness. In addition, titanium bridge connecting between two tops and small crack lines could be generally found (Figure 1).

After installation, discontinuity of surface from chipping of titanium, depression and smooth area were found. Although the top of groovy unit was partially abraded, submicron roughness at the cliff and valley remained underneath the defect (Figure 2).

NO surface showed trapezoid-shaped thread with a ladder step at apical slope. Implant surface demonstrated isotropic micron sized volcano-like structure. At high magnification, the image revealed crater (1-5 μm size) over smooth background with submicron porosity (Figure 1).

After installation, loss of typical volcano-like structure was identified randomly at thread top. Roughness decreased visually. Chipping and distortion at thread crests were found specifically at apical third of the implant in conjunction with crack line (Figure 2).

Table 3 Hounsfield units, cortical bone thicknesses, and torque values of each group

Groups	Hu	Cortical thickness (mm)	Torque value (Ncm)
SU	582.0 ± 2.5	2.4 ± 0.3	31.2 ± 2.5
TS	580.0 ± 23.6	2.5 ± 0.3	31.0 ± 1.4
BP	584.8 ± 19.6	2.5 ± 0.3	33.0 ± 3.4
NO	583.8 ± 32.4	2.4 ± 0.5	29.4 ± 4.8

Mean values ± standard deviations shown.

Remark: SU: (Superline, Dentium, Seoul, Korea)

TS: (TSIII BA, Osstem, Seoul, Korea)BP: (Biomate Plus, Biomate, Kaohsiung, Taiwan)

NO: (Nobel CC, Nobel Biocare, Karlskoga, Sweden)

Hu: Hounsfield unit

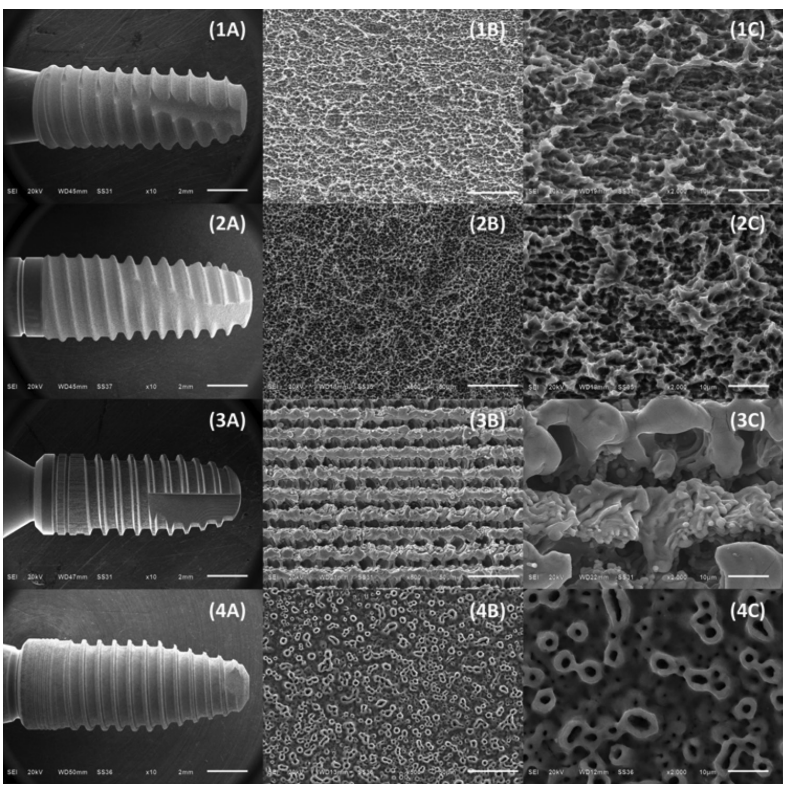

Figure 1 SEM images of all implants

Coloum A-C showed the macroscopic and microscopic view of the implant at 10x , 500x and 2,000x magnificaiton, respectively.

Row 1-4 showed SEM images of SU, TS, BP, and NO implants, respectively.

(1A) Macro geometry showing tapered design with triangular thread shape.

(1B) Smaller pores in larger pores structure.

(1C) Spike-like pattern of SLA surface.

(2A) Macro geometry after sonication showing tapered design with triangular thread shape.

(2B) Smaller pores in larger pores structure.

(2C) Spike-pattern surface.

(3A) Macro geometry showing tapered design and trapezoid thread shape.

(3B) First level roughness of laser modification surface showing groovy pattern along long axis.

(3C) Second level roughness showing micron to submicron roughness and crack lines over the top and cliff of groovy unit.

(4A) Macro geometry showing trapezoid-shaped thread with a ladder step on apical slope.

(4B) Volcano-like structure of anodized surface.

(4C) 1-5 μm sized crater and smooth background with submicron porosity.

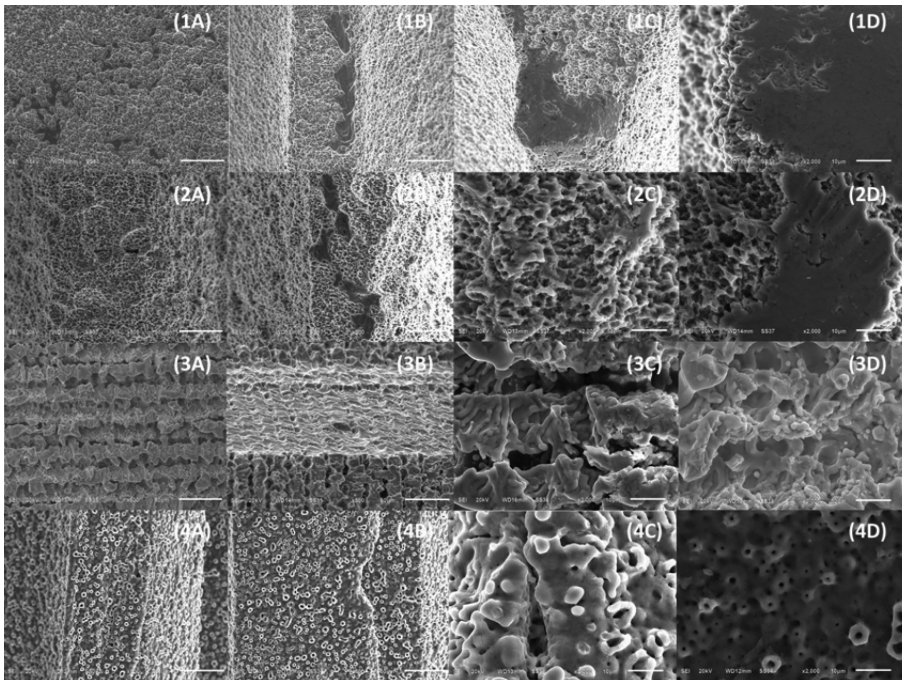

Figure 2 SEM images of all implants after installation into bone block

Coloum A,B showed the macroscopic and microscopic view of the implant at 500x magnification.

Coloum C,D showed the macroscopic and microscopic view of the implant at 2,000x magnification.

Row 1-4 showed SEM images of SU, TS, BP, and NO implants, respectively.

(1A) Decreased sharpness of SLA spike-like pattern.

(1B) Titanium plastic deformation.

(1C,D) Total loss of SLA surface structure.

(2A) Decreased sharpness of SLA spike-like pattern.

(2B) Titanium plastic deformation.

(2C) Partially loss of SLA surface structure.

(2D) Total loss of SLA surface structure.

(3A) Superficial abrasion of surface modification layer.

(3B) Depression on the surface.

(3C) Titanium plastic deformity.

(3D) After superficial abrasion, the roughness below still remained.

(4A) Smoothened surface, deformed thread crest, and crack line.

(4B) Chipping of titanium at thread crest.

(4C) Micro crack line and obstructed volcano nodule.

(4D) Partial loss of typical volcano-like structure.

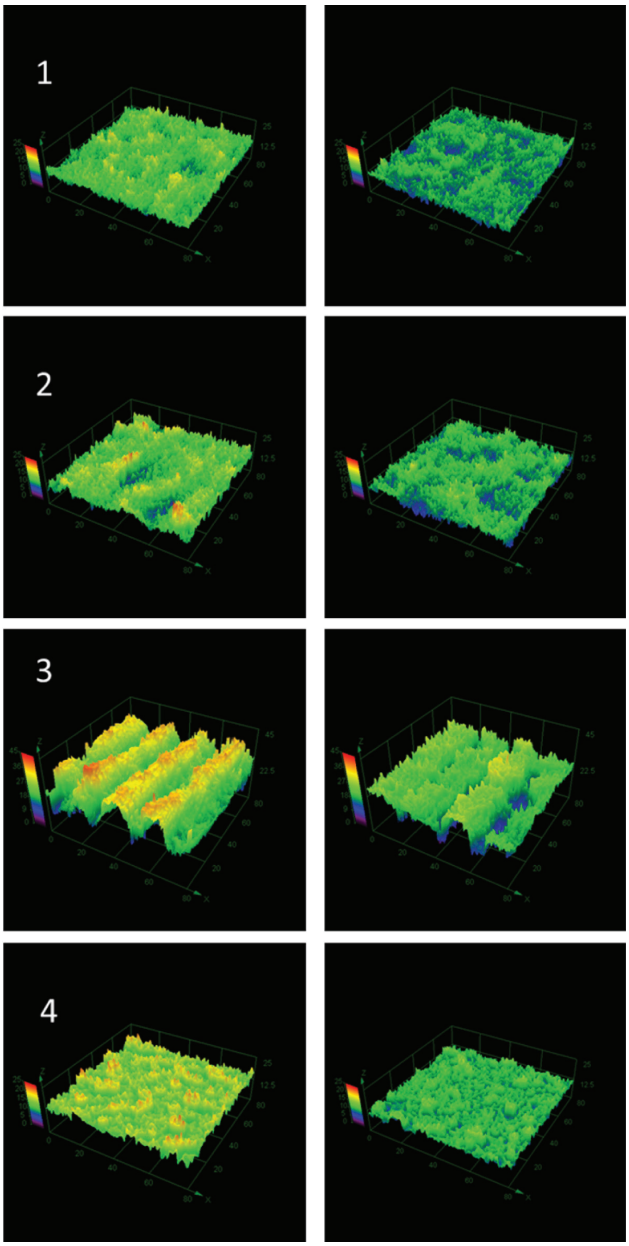

Figure 3 Comparison of topography before (left) and after installation (right) of 4 commercial implants; SU (1), TS (2), BP (3), and NO (4)

Overall, the surface alteration was not remarkable. The thread top and crest were the most affected area. Loss of typical surface modification structure was a major alteration.

Topographical analysis

The results are summarized in (Table 4). 3D topography images are shown in (Figure 3). BP possessed the highest Sa and S-ratio, while NO occupied the lowest Sa and S-ratio. All groups, except NO showed negative Ssk. SLA surface from SU and TS had Sku > 3, indicated inordinately deep valleys. BP and NO had Sku < 3, indicated uniform surface peaks and valleys. BP exhibited a strong long-crestness surface while others presented uniform texture [18].

All implant groups experienced significant decreased Sa and S-ratio. The percentage decrease of S-ratio was generally 4.5-5.5% wherein SU presented the highest percentage decrease (5.5%) and NO presented the lowest percentage decrease (4.5%). Percentage decrease of Sa from BP, SU, TS, and NO was 15, 19, 5, and 2%, respectively. Sku in all groups remained the same. Ssk from SU significantly increased after insertion.

Discussion

Surface modification of dental implant was currently a developing objective to improve an osseointegration [4,9]. Enhancement of topography benefited particularly in the early bone healing process. A rough surface could effectively stimulate cell proliferation and release of biomolecules to initiate angiogenesis and bone formation [19,20]. Moreover, the topography determined protein-surface interaction. A well-modified surface increased surface energy and biomolecule adsorption hastening biological response [21,22].

Nevertheless, the question was raised whether surface physico-chemical properties altered during installation. The change of the topography directly affects those properties. However, direct examination of the physico-chemical properties after installation is unreliable because contamination and cleaning process directly influence surface chemistry. Therefore, indirect investigation using the topography alteration might be reasonable option.

Table 4 Surface topography of implants before and after installation

Implant system	Parameters	Control	After installation	*p*-value
SU	S-ratio	3.27 ± 0.28	3.12 ± 0.33	<0.001[a)]
	Sa (μm)	1.89 ± 0.40	1.54 ± 0.32	<0.001[a)]
	Ssk	-0.12 ± 0.22	-0.01 ± 0.27	0.002[a)]
	Sku	3.08 ± 0.22	2.97 ± 0.65	0.081
	Str	0.47 ± 0.19	0.49 ± 0.18	0.148
TS	S-ratio	3.65 ± 0.85	3.45 ± 0.51	<0.001[a)]
	Sa (μm)	2.08 ± 0.34	1.97 ± 0.28	<0.001[a)]
	Ssk	-0.10 ± 0.24	-0.02 ± 0.26	0.061
	Sku	3.49 ± 0.78	3.55 ± 0.92	0.181
	Str	0.47 ± 0.25	0.51 ± 0.22	0.158
BP	S-ratio	4.46 ± 0.38	4.24 ± 0.41	<0.001[a)]
	Sa (μm)	5.21 ± 0.77	4.41 ± 0.94	<0.001[a)]
	Ssk	-0.40 ± 0.20	-0.36 ± 0.23	0.456
	Sku	2.49 ± 0.33	2.90 ± 0.91	0.194
	Str	0.18 ± 0.03	0.20 ± 0.10	0.253
NO	S-ratio	2.91 ± 0.30	2.78 ± 0.19	<0.001[a)]
	Sa (μm)	1.37 ± 0.14	1.34 ± 0.13	0.041[a)]
	Ssk	0.30 ± 0.16	0.28 ± 0.27	0.472
	Sku	2.99 ± 0.54	3.03 ± 0.94	0.579
	Str	0.74 ± 0.18	0.77 ± 0.14	0.262

Mean values ± standard deviations shown.

[a)] significant difference from control ($P < 0.05$).

Remark: SU: (Superline, Dentium, Seoul, Korea)
TS: (TSIII BA, Osstem, Seoul, Korea)
BP: (Biomate Plus, Biomate, Kaohsiung, Taiwan)
NO: (Nobel CC, Nobel Biocare, Karlskoga, Sweden)

Plastic deformity of titanium surface during installation were described as a phenomenon of shear stress during the rough titanium surface compressed against cortical and trabecular bone [13,23]. The current study suggested factors which influenced the alteration including three major factors; properties of implant, bone, and insertion force. The dental implants were often produced from grade IV, grade V titanium or zirconia [5]. Different materials had different mechanical properties, for instance a commercial pure titanium had lower surface hardness than titanium alloy [24].

Surface hardness was a factor that played an important role in surface abrasion which high surface hardness hypothetically tolerated to the abrasion [8,25]. Moreover, implant macroscopic designs were various such as conical, tapered, self-threading design, hence they displayed different force distribution during installation. For example, self-threading implant used its threads to cut the bone, therefore the stress was more concentric to those threads [11].

The shape and size of implant along with the shape of a final drill also indicated the tightness and stress distribution during installation [11]. The

bony implant bed could be prepared using the final drill as termination or combining with a cortical bone drill and tap, depended on bone type. Somehow, the cortical bone drill and tap were optionally used upon a clinician preference, thus misjudgment and inadequate implant bed preparation would lead to difficulty of insertion, high insertion torque demand and, extensive surface damage.

Bone density can be ranged from very soft to hard bone depended on the density of trabeculae pattern and cortical bone thickness [26]. The denser trabecular architecture could increase the area of implant-bone contact during the installation. Likewise, the cortical bone is very dense component which is hypothesized to give highest surface damage when the implant contacts bone. The thicker cortical layer would allow the greater surface area of implant-bone contact. Hence, the implant surface breakdown might be greater with denser and harder bone [6,11].

Experimental design was carefully developed to achieve accurate result and reflect clinical scenario. The porcine pelvic was used as a model in this study because it has the cortical bone thickness 0.5-2.5 mm and similar trabeculae pattern to human [27]. Standardized bone samples using Hu and cortical bone thickness allowed the consistent experiments.

CT was a promising method for quantitative bone density assessment because Hu was well-standardized and constant [28]. According to bone block assessment result, D3 bone type (Misch classification) was presented [26]. Furthermore, because this study intended to mimic ideal clinical scenario, implant placement was strictly done following the manufacturer recommendations with appropriated torque.

The force being used during installation depended on the torque value. Higher torque generated more force that allowed the implant to squeeze the surrounding bony socket to a correct position [29]. High insertion force would also lead to greater mechanical change to the surface. Regarding all these factors, tendency for surface alteration might be predicted.

In the previous articles, to investigate surface structure after installation in either bone or plastic block, the removal of residual bone and particle was very crucial to unmask underneath surface. The previous studies reported an incomplete removal of residual, hence this directly affected the findings [15,28]. In this study, the sonication under distilled water and acetone were adequate for bone residual removal.

After installation, all implants experienced surface alteration especially thread top and thread crest manifested as loss or deformation of titanium. The thread top and crest experienced greater damage because they were outermost and had greater chance to contact the bone [11]. This study concluded that the alteration under SEM was random and sparse.

SLA surface was found to be most affected from the installation process similar with a previous study which smooth area generally appeared over the surface [13]. This result might be explained by the microstructure of SLA surface which consisted of typically sharp asperities. Interestingly, laser treated and anodized surface tolerated alteration more than the SLA surface. Laser treated surface consisted of deep groovy structure. Although the outermost layer of surface modification was abraded, the roughness over cliff and valley remained. In addition, anodized surface did not consist of sharp asperity, thereafter the abrasion was minimal.

Investigation under SEM was only based on investigator perception. To quantify the alteration, topography study was necessary. There were various topographical parameters in Metrology. Wennerberg recommended at least one parameter from all these three categories; height, spatial, and hybrid. In addition, combination of measurement at top, flank, and valley at least 9 regions of interest for each implant was adequate to represent

topography data [7]. The present study selected Sa, Sku, Ssk, and Str for height and spatial parameters. However, software Lext1.1.3 was not be able to calculate Sdq or Sdr which were frequently used as hybrid parameters. The current study proposed a similar parameter called "S-ratio" which it mathematical definition is close to Sdr. It represented a proportion of true surface area to cross-sectional surface without effect from the filter.

This study found decreased Sa and minimal change of Ssk, Sku, and Str in all implants after installation, which were similar to previous studies [13,14,23]. SU was observed to have the most decreased Sa and S-ratio. This observation was explained by the spike surface over micro pores from blasting process causing large surface contact to surrounding bone during installation. Compared with TS, the surface was constructed with more aggressive blasting, consequently it consisted deeper and larger micro pores which allowed less surface contact to the bone.

On the contrary, NO was least changed because it consisted relatively of flat structure compared to other surfaces. Moreover, for BP surface, despite of dominant decrease of Sa, the S-ratio was slightly altered. This result might be the exposure of submicron roughness which could not identified previously because laser beam was not be able to illustrate submicron roughness over the cliff and with deep valley.

The current commercial implants are various. Different implants manifest alteration individually. Although, the dental implant was installed following a manufacture guideline strictly, the alteration of surface was still presented. Hypothetically, more aggressive implant installation such as high torque insertion and multiple placement would cause more damage to the surface. The alteration should be minimized to transfer the constructing surface properties to an oral cavity as much as possible. This result should also be regarded for future implant macroscopic and microscopic designs. Other studies relate surface topography to other factors might consider the topographical change for more intimate clinical implication. The limitations of this study, the relation between surface alteration and the other factors such as different bone types, the macro designs, or the installation torques has not yet investigated. In addition, investigation effect of surface alteration on clinical success of the implant can be future goal.

Conclusions

Surface alteration after installation was proved in the present study. The morphological alteration was visible under SEM in all implant surfaces. All implant surfaces showed significant topography change, especially height parameter and surface area.

Acknowledgement

The authors would like to thank the staff and dental assistants including colleagues and co-workers in the Department of Oral and Maxillofacial Surgery, Faculty of Dentistry, Mahidol University.

Ethics approval: All animal experiments were approved by the Mahidol University-Institutional Animal Care and Use Committee (license MU-IACUC 2019/005).

Availability of data and materials: The datasets used and analyzed during the current study are available from the corresponding author on reasonable request.

Competing interest: The authors declare that they have no competing interests.

Funding: None

References

1. Elias CN, Rocha FA, Nascimento AL, Coelho PG. Influence of implant shape, surface morphology, surgical technique and bone quality on the primary stability of dental implants. *J Mech Behav Biomed Mater* 2012; 16: 169-80.
2. Coelho PG, Granato R, Marin C, Teixeira HS, Suzuki M, Valverde GB, et al. The effect of different implant macrogeometries and surface treatment in early biomechanical fixation: an experimental study in dogs. *J Mech Behav Biomed Mater* 2011; 4: 1974-81.
3. Abuhussein H, Pagni G, Rebaudi A, Wang HL. The effect of thread pattern upon implant osseointegration. *Clin Oral Implants Res* 2010; 21: 129-36.
4. Almas K, Smith S, Kutkut A. What is the Best Micro and Macro Dental Implant Topography? *Dent Clin North Am* 2019; 63: 447-60.
5. Smeets R, Stadlinger B, Schwarz F, Beck-Broichsitter B, Jung O, Precht C, et al. Impact of dental implant surface modifications on osseointegration. *Biomed Res Int*. 2016; 6285620.
6. Yalçın M, Kaya B, Laçin N, Arı E. Three-Dimensional Finite Element Analysis of the Effect of Endosteal Implants with Different Macro Designs on Stress Distribution in Different Bone Qualities. *Int J Oral Maxillofac Implants* 2019; 34: 43–50.
7. Wennerberg A, Albrektsson T. Suggested guidelines for the topographic evaluation of implant surfaces. *Int J Oral Maxillofac Implants* 2000; 15: 331-44.
8. Albrektsson T, Wennerberg A. Oral implant surfaces: Part 1--review focusing on topographic and chemical properties of different surfaces and in vivo responses to them. *Int J Prosthodont* 2004; 17: 536-43.
9. Shibli JA, Grassi S, de Figueiredo LC, Feres M, Marcantonio E Jr, Iezzi G, et al. Influence of implant surface topography on early osseointegration: a histological study in human jaws. *J Biomed Mater Res B Appl Biomater* 2007; 80: 377-85.
10. Zhu X, Chen J, Scheideler L, Reichl R, Geis-Gerstorfer J. Effects of topography and composition of titanium surface oxides on osteoblast responses. *Biomaterials* 2004; 25: 4087-103.
11. Guan H, Van Staden RC, Johnson NW, Loo Y-C. Dynamic modelling and simulation of dental implant insertion process—A finite element study. *Finite Elem Anal Des* 2011; 47: 886-97.
12. Franchi M, Bacchelli B, Martini D, De Pasquale V, Orsini E, Ottani V, et al. Early detachment of titanium particles from various different surfaces of endosseous dental implants. *Biomaterials* 2004; 25: 2239-46.
13. Senna P, Antoninha Del Bel Cury A, Kates S, Meirelles L. Surface damage on dental implants with release of loose particles after insertion into bone. *Clin Implant Dent Relat Res* 2015; 17: 681-92.
14. Menezes HHM, Naves MM, Costa HL, Barbosa TP, Ferreira JA, Magalhães D, et al. Effect of Surgical Installation of Dental Implants on Surface Topography and Its Influence on Osteoblast Proliferation. *Int J Dent* 2018; 4089274.
15. Pettersson M, Pettersson J, Molin Thorén M, Johansson A. Release of titanium after insertion of dental implants with different surface characteristics–an ex vivo animal study. *Acta Biomater Odontol Scand* 2017; 3: 63-73
16. Salerno M, Itri A, Frezzato M, Rebaudi A. Surface microstructure of dental implants before and after insertion: An in vitro study by means of scanning probe microscopy. *Implant Dent* 2015 ; 24: 248-55.
17. Sridhar S, Wilson Jr TG, Valderrama P, Watkins-Curry P, Chan JY, Rodrigues DC. In vitro evaluation of titanium exfoliation during simulated surgical insertion of dental implants. *J Oral Implantol* 2016; 42: 34-40.
18. Liam Blunt KS, Dong W, Mainsah E, Luo N, Mathia T, Sullivan P, et al. Development of methods for the characterisation of roughness in three dimensions. London: Butterworth/Heinemann; 2006.
19. Hotchkiss KM, Reddy GB, Hyzy SL, Schwartz Z, Boyan BD, Olivares-Navarrete R. Titanium surface characteristics, including topography and wettability, alter macrophage activation. *Acta Biomater* 2016; 31: 425-34.
20. Marinucci L, Balloni S, Becchetti E, Belcastro S, Guerra M, Calvitti M, et al. Effect of titanium surface roughness on human osteoblast proliferation and gene expression in vitro. *Int J Oral Maxillofac Implants* 2006; 21: 719-25.
21. Bagno A, Di Bello C. Surface treatments and roughness properties of Ti-based biomaterials. *Int J Oral Maxillofac Implants* 2004; 15: 935-49.
22. Ogawa ES, Matos AO, Beline T, Marques IS, Sukotjo C, Mathew MT, et al. Surface-treated commercially pure titanium for biomedical applications: Electrochemical, structural, mechanical and chemical characterizations. *Mater Sci Eng C Mater Biol Appl* 2016; 65: 251-61.

23. Streckbein P, Wilbrand JF, Kahling C, Pons-Kuhnemann J, Rehmann P, Wostmann B, et al. Evaluation of the surface damage of dental implants caused by different surgical protocols: an in vitro study. ***Int J Oral Maxillofac Surg*** 2019; 48: 971-81.
24. da Rocha SS, Adabo GL, Henriques GE, Nobilo MA. Vickers hardness of cast commercially pure titanium and Ti-6Al-4V alloy submitted to heat treatments. ***Braz Dent J*** 2006; 17: 126-9.
25. Goddard J, Wilman H. A theory of friction and wear during the abrasion of metals. ***Wear***. 1962; 5: 114-35.
29. Misch CE. Bone classification, training keys to implant success. ***Dent Today*** 1989; 8: 39-44.
27. Nienkemper M, Santel N, Hönscheid R, Drescher D. Orthodontic mini-implant stability at different insertion depths. ***J Orofac Orthop***. 2016; 77: 296-303.
28. Choi YJ, Jun S, Song YD, Chang MW, Kwon J. CT Scanning and Dental Implant, CT Scan - Tech and App. 2011.
29. Goswami M, Kumar M, Vats A, Bansal A. Evaluation of dental implant insertion torque using a manual ratchet. ***Med J Armed Forces India*** 2015; 71: 327-32.